
Hippocampus Temporal Lobe Epilepsy Detection Using a Combination of Shape-based Features and Spherical Harmonics Representation

Zohreh Kohan ·
Hamidreza Farhidzadeh ·
Reza Azmi ·
Behrouz Gholizadeh

Abstract Most of the temporal lobe epilepsy detection approaches are based on hippocampus deformation and use complicated features, resulting, detection is done with complicated features extraction and pre-processing task. In this paper, a new detection method based on shape-based features and spherical harmonics is proposed which can analysis the hippocampus shape anomaly and detection asymmetry. This method consisted of two main parts; (1) shape feature extraction, and (2) image classification. For evaluation, HFH database is used which is publicly available in this field. Nine different geometry and 256 spherical harmonic features are introduced then selected Eighteen of them that detect the asymmetry in hippocampus significantly in a randomly selected subset of the dataset. Then a support vector machine (SVM) classifier was employed to classify the remaining images of the dataset to normal and epileptic images using our selected features. On a dataset of 25 images, 12 images were used for feature extraction and the rest 13 for classification. The results show that the proposed method has accuracy, specificity and sensitivity of, respectively, 84%, 100%, and 80%. Therefore, the proposed approach shows acceptable result and is straightforward also; complicated pre-processing steps were omitted compared to other methods.

Keywords temporal lobe epilepsy · spherical harmonics · hippocampus shape-based features · classification · SVM

1 Introduction

In some of the neurological diseases one or more brain components and substructures are affected. Some of these effects deform the shape of those components in

Z.Kohan · R.Azmi · B.Gholizadeh
Department of Computer Engineering, Alzahra University, Tehran, Iran

*Corresponding Author :H.Farhidzadeh
Department of Computer Science and Engineering,
University of South Florida,
Tampa, FL, USA
E-mail: hfarhidzadeh@mail.usf.edu

one of the brain hemisphere or both. Therefore, unilateral and/or bilateral shape analysis of brain structures could lead to a better understanding of the abnormalities. There are evidences in the literature [1,2,3,4] showing that the brain structures deform when some diseases such as schizophrenia, Alzheimers, Parkinson, and epilepsy occur. So using precise representation is helpful to parameterize the deformation that will be useful to diagnosis of the mentioned illnesses automatically. Hippocampus is a brain structure that belongs to the limbic system and is located in the medial temporal lobe. Hippocampus plays an important role in the formation of declarative, emotional, and long-term memories as well as language processing [5]. Hippocampus is one of the main targets of deformation in the brain in some disorders such as temporal lobe epilepsy. So, 3D representation and analysis of this structure could be useful in prognosis and diagnosis of those types of diseases. To characterize the deformation of the brain structures volumetric [6] or shape analysis is used. Volumetric analysis is easy to interpret deformation but shape analysis is more common because of its ability in geometric and morphometric features description. There are two groups of approaches used for shape representation; explicit and implicit shape representation. In explicit representation, the shape is illustrated as a parametric form and in implicit representation it represents as the level set of a scalar function. There are some examples of shape analysis methods in the literature in which either implicit or explicit shape representation is used. Statistical analysis of the anatomical shape deformations, which occur in epilepsy and other neurological disorders, require both global and local parameter based characterization of the anatomical shape that is deformed. Size- and volume- based analysis is the most popular method to achieve the parameterization of the shape deformations[8,9]. Many methods are proposed to analyze hippocampus are needed complicated pre-processing task. Most of them are reviewed in[8,9,10,11]. Since many of the shape-based features can illustrate hippocampus deformation and employ for detection. These features are straightforward and avoid complicated pre-processing steps. This method utilized spherical harmonics (SPHARM) that is a powerful mathematical tool that is used for representation and analysis of 3D closed surfaces [15]. SPHARM can be utilized in 3D representation and analysis of the brain structures. However, in contrast to previous studies on hippocampus shape analysis using SPHARM-Based shape descriptor, this work has been focused on the detection of asymmetry in hippocampus shape using SPHARM coefficients as the shape features. A subset of the coefficients that were able to detect the asymmetry in left and right hippocampus was used to classify the images into either normal or epilepsy patient groups. Moreover, the complexity of this method is less compared to the other presented methods. As a result, in this paper, combination of shape-based features and spherical harmonics, this proposed method can analyze hippocampus shape and diagnose temporal lobe epilepsy in MR images.

2 PREVIOUS WORKS

Shen et al. [7] have reported about deformation of the hippocampus in epilepsy patients. The deformation of hippocampus has led the research groups to study the shape of the hippocampus for diagnosis purposes. Gerig et al. [8] to analyze hippocampal shape use volume measurements and shape-based features. Shape-

based feature that is used is based on Mean Square Distance (MSD) between left and right hippocampus surface shapes. Then Support Vector Machines (SVM) is employed to classify, also leave- one-out cross validation is applied to evaluation performance. Csernansky et al. [9] used registration to compare the hippocampal volume and shape characteristics in patient and control subjects. Computing transformation vector from the points on the hippocampus surface represents shape. Kodipaka et al. [10] used the Kernel Fisher Discriminant (KFD) algorithm for shape-based classification of hippocampal shapes. In this method, some landmarks manually placed on the hippocampus surface by an expert that indicated boundaries of the shape, then feature extraction is done by fitting a model to the landmarks using a deformable pedal surface, see detail about a deformable pedal surface in [13]. The result of this fitting process is a smooth surface that used in similarity alignment followed by a level-set non-rigid registration that describe in [14]. The output of this registration is local deformation between left and right hippocampus that used as input to the Kernel Fisher classifier. Esmailzadeh et al. employed spherical harmonics (SPHARM) to analysis hippocampus shape [11]. This method alignment hippocampus left and right to each other the extract features based on spherical harmonic confidents, finally using SVM for calssification. Shishegar et al. have used Laplace Beltrami operator for TLE diagnosis [12]. This method proposed a feature vector that described size and shape based on Laplace Beltrami eigenvalues and eigen-functions. Some of pervious methods need registration as pre- processing step [6,7,8]. Also in [10] using shape alone could not capture shape differences. Furthermore the most of reviewed methods is complicated and need pre-processing step. In this paper, a new method is presented that using straightforward shape-based features for detection and omitted complicated pre-processing step such as registration.

3 THE PROPOSED METHOD

The purposed method has two parts for feature extraction. In each part using statistical t-test most significant features is selected. Then a main feature vector is formed. Finally SVM is employed for classification hippocampus shapes. Fig.1 illustrate block diagram of the purposed method.

3.1 Materials

Our dataset contained 25 T1-weighted coronal brain MR images (MRI) from Henry Ford hospital. MRI data is very useful for imaging in different applications such as breast cancer [28] and sarcomas [29]. 20 of the images were acquired from temporal lobe epilepsy subjects with medically intractable seizures and the remaining five were from normal subjects used as control dataset. Ten images out of 25 (all from epilepsy patients) were acquired with 1.5 Tesla MRI scanners and the remaining ones (15 images from epilepsy patients and all the normal cases) were from 3.0 Tesla MRI scanners. Slice thickness of all the images was 2.0 mm and the 2015, in-plane resolution of the pixels varied from $0.39 \times 0.39mm$ to $0.75 \times 0.75mm$. For each image one expert provided a manual segmentation, then the segmentation labels were reviewed and confirmed by two more experts.

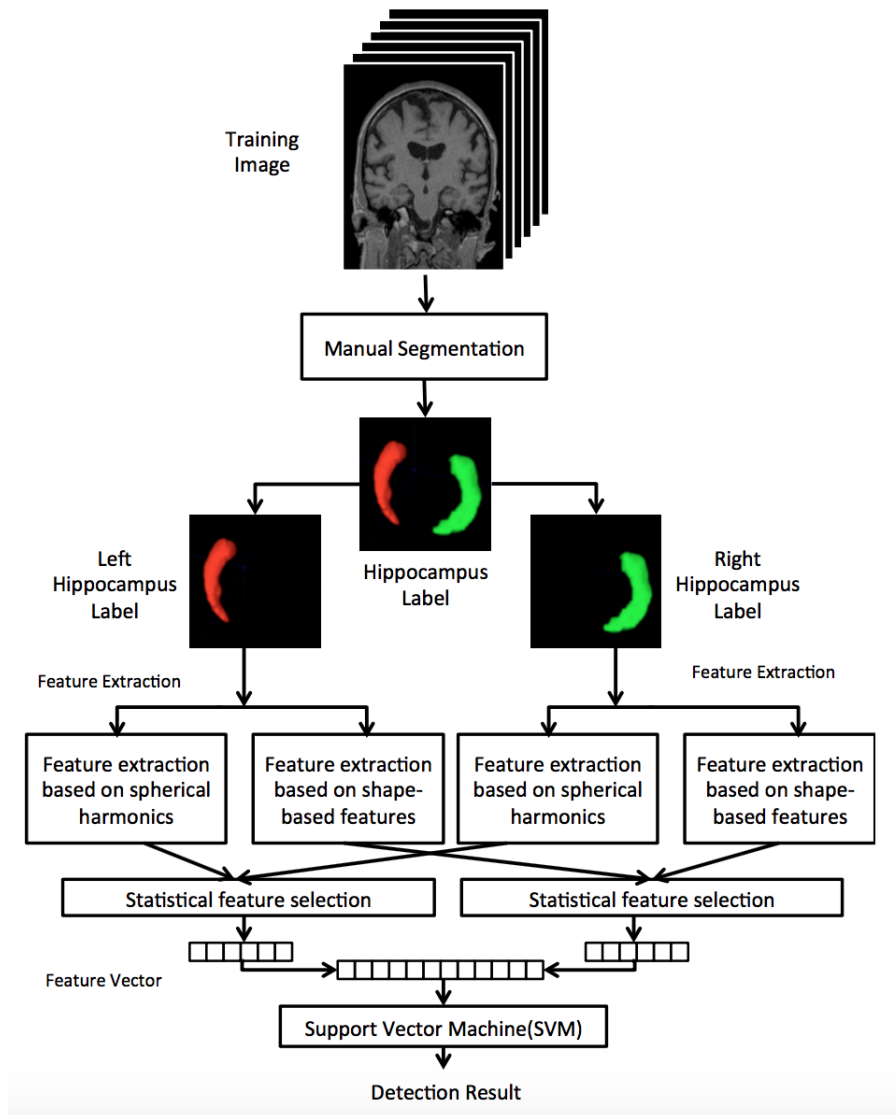


Fig. 1 Purposed method block diagram

3.2 Feature extraction based on spherical harmonics

This part consists of pre processing steps that explained below.

3.3 Surface meshing

To generate a surface mesh for hippocampus shape, first, 3D manual segmentation was applied. For the further shape analysis and also for the classification of the hippocampus structure, it was necessary to have a mathematical representation of the 3D structure. One of the most common and simplest representations for explicit representation of the 3D surfaces is triangulation. In this method the shape is represented as a set of 3D discrete points that connected via triangular mesh. The marching cube algorithm [26] is a popular triangulation method applied to a 3D surface to obtain triangle surface mesh. After applying marching cube algorithm, the 3D shape is represented by coordinates of triangle mesh vertices as:

$$X = [x_1, y_1, z_1, \dots, x_n, y_n, z_n]^T \quad (1)$$

Where n is the number of vertices.

3.4 Spherical parametrization

First step in SPHARM representation is mapping the 3D surface to unit sphere under bijective mapping with lower distortion in area and topology called spherical parameterization [25]. This mapping is applied to a 3D surface represented as a triangular mesh. After mapping the surface mesh on the unit sphere each vertices can be represented in spherical polar coordinate with two parameters, the inclination angle θ and the azimuth angle φ .

In this paper, for spherical parametrization we use, CALD algorithm that proposed by Shen and Makedon [26]. This algorithm consists of two steps: first, initial parametrization for triangular mesh [25] and second, local smoothing and global smoothing parametrization improve the quality of the parametrization. The goal of local smoothing step is minimization of the area distortion at a local sub mesh, this goal is achieved by solving a linear system and controlling its worst length distortion simultaneously. The global smoothing step as the second step of the algorithm compute the distribution of the surface distortions for all the mesh vertices, to equalize them over the complete sphere. In an overall view, the CALD algorithm merges the local and global methods together and executes each method alternately until a best parametrization is achieved. Fig.2 shows the left part of a hippocampus mapped to the unit sphere through this 3D mapping approach.

3.5 SPHARM analysis

The SPHARM is a powerful mathematically tool that used for representation and analysis of 3D closed surface. The overall SPHARM analysis includes three main steps:

- Surface meshing
- Surface parametrization
- Spherical expansion

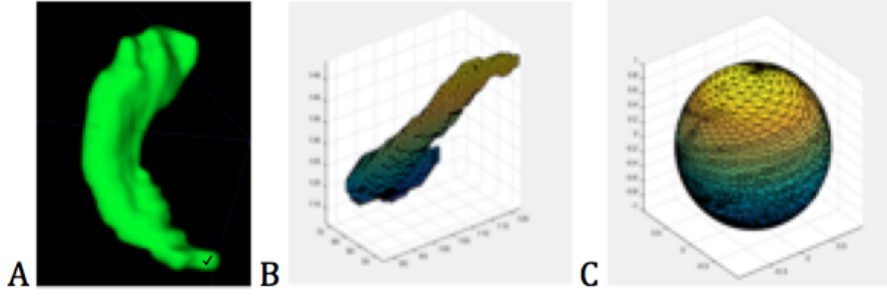


Fig. 2 A) Left hippocampus. B) The result of marching cube meshing algorithm. C) The result of spherical parameterization

The first two steps have been explained in section II.C. When the 3D surface is represented via two parameters (the inclination angle θ and the azimuth angle φ) the surface can be expanded into a complete set of SPHARM basis functions Y_l^m .

$$Y_l^m(\theta, \varphi) = \sqrt{\frac{2l + l(1 - m)!}{4\pi(1 + m)!}} p_l^m \cos(\theta) e^{im\varphi} \quad (2)$$

where

$$0 < l < L_{max}$$

and

$$-l < m < l$$

and $p_l^m \cos(\theta)$ is the associated Legendre polynomials defined by the differential equation as follows:

$$P_l^m(x) = \frac{(-1)^m}{(2^i l!)} (1 + x^2)^{m/2} \frac{(d^{l+m})}{(dx^{l+m})} (x^2 - 1)^l \quad (3)$$

The surface is independently decomposed through SPHARM as:

$$x(\theta, \varphi) = \sum_{l=0}^{L_{max}} \sum_{m=-l}^l C_{lx}^m Y_l^m(\theta, \varphi) \quad (4)$$

$$y(\theta, \varphi) = \sum_{l=0}^{L_{max}} \sum_{m=-l}^l C_{ly}^m Y_l^m(\theta, \varphi) \quad (5)$$

$$z(\theta, \varphi) = \sum_{l=0}^{L_{max}} \sum_{m=-l}^l C_{lz}^m Y_l^m(\theta, \varphi) \quad (6)$$

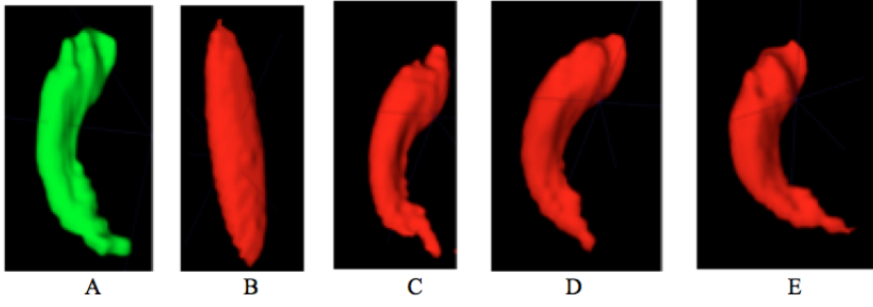


Fig. 3 A) 3D shape of left hippocampus and (B-E) its reconstruction through SPHARM based shape reconstruction using (B) $L - max=1$ (C) $L - max =8$ (D) $L - max =16$ and (E) $L - max =24$

These terms can be combined into a single function:

$$v(\theta, \varphi) = \sum_{l=0}^{L_m ax} \sum_{m=-l}^l C_l^m Y_l^m(\theta, \varphi) \quad (7)$$

Where

$$v(\theta, \varphi) = (x(\theta, \varphi), y(\theta, \varphi), z(\theta, \varphi))^T \quad (8)$$

And

$$C_l^m = (C_{lx}^m, C_{ly}^m, C_{lz}^m)^T \quad (9)$$

The coefficients C_l^m are computed using least-squares estimations. According to equation (7) these coefficients are determined up to user-desired maximum degree $L_m ax$.

The original surface is indicated as $X = (x_1, x_2, x_3, \dots, x_n)^T$ and $(a_1, a_2, a_3, \dots, a_k)$ is an estimate for the coefficients which are Featureselection obtained by solving previous equation follow manner:

$$C_l^m \cong Y_l^{mT} Y_l^m^{-1} X \quad (10)$$

As claimed by equation (7), after coefficients are estimated, the 3D surface can be reconstructed. Fig.3 illustrates reconstruct shape in four different degrees using higher degrees yield to more details in the reconstructed shape.

3.6 Featureselection

The real parts of SPHARM coefficients were used as features in this work. For each subject hippocampus has two parts; left and right. For each part the coefficients were computed up to degree 15. So the length of feature vector is $3 \times (15+1)^2 = 768$ for each side. To make the coefficients comparable across left and right hippocampus, we needed to normalize them by cancelling out the translational and rotational misalignments. Rotation was achieved by alignment of reconstructed shape based on first degree coefficients only (i.e. an ellipse). We used the alignment algorithm

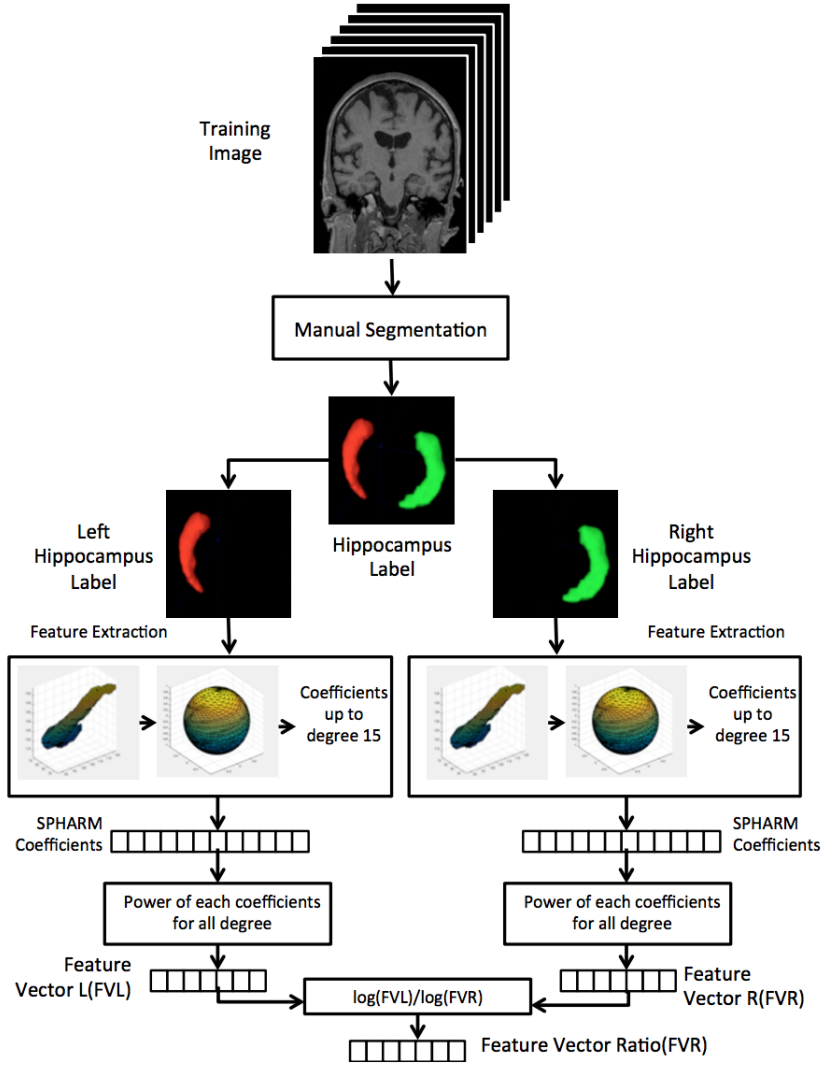


Fig. 4 Feature extraction

that used in [26]. For that purpose we aligned the shortest and the longest axis of the ellipse along x-axis and z-axis, respectively. We also translated the shapes to the origin of the coordinate system by ignoring the coefficients of degree 0. Since we used the ratio of left and right coefficients for each hippocampus, no scaling adjustment was required. After normalizing the coefficients, we calculated sum of the power of each coefficients for all the degrees as shown in equation (11).

$$\left(\sqrt{\sum_{m<|l|} \|C_0^m\|^2}, \sqrt{\sum_{m<|l|} \|C_1^m\|^2}, \sqrt{\sum_{m<|l|} \|C_2^m\|^2}, \dots, \sqrt{\sum_{m<|l|} \|C_l^m\|^2} \right) \quad (11)$$

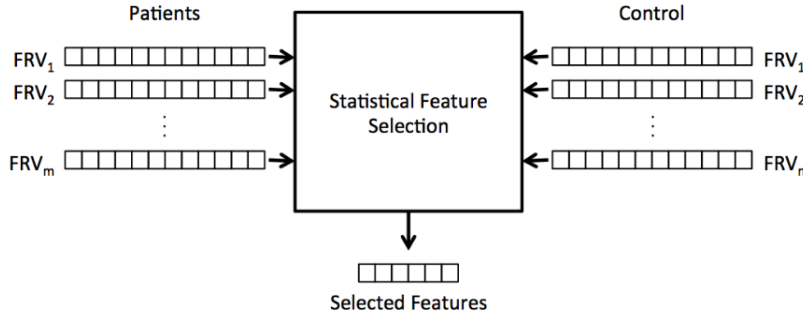


Fig. 5 Feature extraction

This step yielded to a feature vector of $(15 + 1)^2 = 256$ elements. Since our aim was to detect hippocampal asymmetry we calculated the ratio of logarithm of left coefficients to logarithm of right coefficients. We used logarithm to make the features of different orders more comparable.(Fig.4)

Since only some of the listed features carried applicable information for the classification of shape (significantly differentiate between normal and abnormal shapes), we employed a statistical t-test to identify and select the most discriminative features. Fig.5 shows a schematic diagram of the feature selection algorithm. We run t-test on the each element (feature) of features vector to compare the element values of patients and normal subjects in a training set. For two sets of samples (in this paper one set is the feature values for normal cases and the second set is the feature values for the epilepsy cases) with averages of M1 and M2 the p-value indicates the probability that the observed difference between M1 and M2 is due to chance under the null hypothesis that M1 and M2 are the same. Therefore, a lower p-value shows statistically stronger difference that corresponds to a more significant feature. We obtained the associated p-value for each feature and selected those features with p-values of less than 0.05 as significantly discriminative features. Our hypothesis was that the significant features could help better in classification of hippocampus into healthy and epileptic classes. To select the best features that are able to differentiate between normal and epileptic subjects, first we randomly selected a subset of 12 images from our data set to form our training set. The training set contained both normal (two images) and epileptic (ten images) subjects. The remaining images were used as the test dataset in the classification explained in the next subsection. We extracted all SPHARM coefficients then created the feature vectors as described; we used t-test to select those features in which the value of the feature between normal and patient cases was detected significantly different ($p - value < 0.05$).

3.7 Feature extraction based on shape-based features

In this section we first introduced all the features we used to study shape characteristics. Table 1 shows a list of shape and size features we have used in this project to detect asymmetry between right and left hippocampus. Fig.6 shows a

Table 1 Shape-based features and corresponding p-values

Feature	p-value
Maximum shape diameter	0.7187
Shape volume	2.54×10^{-4} **
Surface area	0.7690
Compactness[26]	0.7054
Mesh size	0.0015**
First-order border moments[25]	2.38×10^{-4} **
Third-order border moments[25]	0.5088
Circumscribed sphere volume to shape volume ratio	0.6028
Curvature	0.075*

general block diagram of our feature extraction method. Following we described these features.

3.7.1 Maximum shape diameter

The maximum possible Euclidian distance between two points of the surface of the shape. Since epilepsy disease could deform the surface of the hippocampus [25] it might changes maximum diameter of the shape.

3.7.2 Shape volume

To measure the shape volume of right and left hippocampus we multiply number of voxels by the volume of a single voxel. Surface area: To measure the surface area we calculated the summation of the outer surfaces of all the voxels that formed the hippocampus surface.

3.7.3 3D Compactness

Compactness is a unit less shape feature that describes how closely packed the shape is. In the other hand, it shows the roughness of a shape surface to its volume [26]. Sphere has the smallest value of 3D compactness i.e. about 113. As the sphere deforms towards a more complicated shape, compactness becomes larger and larger. 3D compactness (C) calculated as ratio of the cubed surface area (A) to the squared surface volume (V):

$$C = \frac{A^3}{V^2} \quad (12)$$

3.7.4 Mesh Size

In this paper we measured the number of vertices in the shape surface mesh using marching cube meshing algorithm [26]. The marching cubes algorithm is a 3D iso-surface representation technique for generating mesh for a 3D surface.

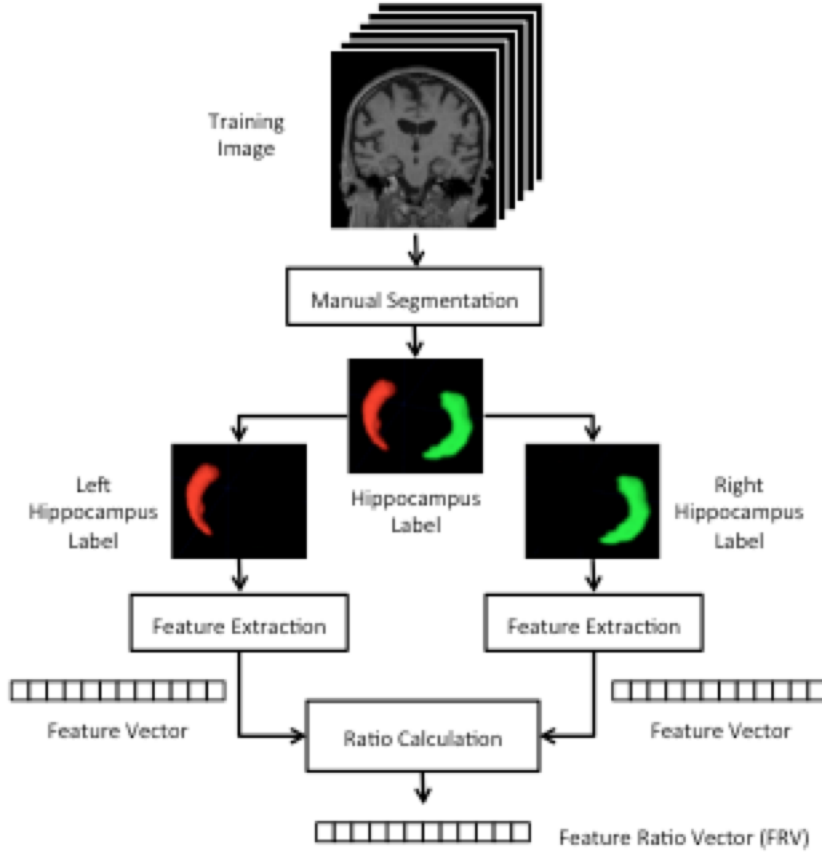


Fig. 6 Feature extraction

3.7.5 Moments

Moments are the statistical property of the shape that are evolved from the moment concept in physics. There are two types of moments, region moments and boundary moments. In this work, we use boundary moments [25]. The p th moment is defined as:

$$m_p = \frac{1}{N} \sum_{i=1}^N [z(i)]^p \quad (13)$$

where $d(i)$ is Euclidian distance between i th voxels and the centroid, N is number of voxels. The p th central moment defined as:

$$M_p = \frac{1}{N} \sum_{i=1}^N [z(i) - m_1]^p \quad (14)$$

In this paper we use low-order moments such as M1 and M3 that are defined as below:

$$F_1 = \frac{[\frac{1}{N} \sum_{i=1}^N [z(i) - m_1]^2]^{\frac{1}{2}}}{\frac{1}{N} \sum_{i=1}^N z(i)} \quad (15)$$

and

$$F_3 = \frac{[\frac{1}{N} \sum_{i=1}^N [z(i) - m_1]^4]^{\frac{1}{4}}}{\frac{1}{N} \sum_{i=1}^N z(i)} \quad (16)$$

where

$$m_1 = \frac{1}{N} \sum_{i=1}^N z(i) \quad (17)$$

3.7.6 Circumscribed sphere volume to shape volume ratio

This is the ratio of the volume of the circumscribed sphere centred at the shape centroid to the volume of the shape.

3.7.7 Curvature

We defined the curvature of the shape as follows:

$$C = \frac{d_{C1} + d_{C2}}{d_{12}} \quad (18)$$

Where d_{C1} and d_{C2} are the Euclidian distances between centroid of the shape and two opposite tips of the shape that are located in the maximum distances to the centroid and d_{12} : is the Euclidian distance between the two tips of the shape. To analysis the shape and size of the left and right hippocampus, we extracted all the features for left and right hippocampus, separately. Then we measured the ratio of right feature values to left feature values as well as left feature values to right. We chose the ratio that is greater or equal to 1 as an indicator for hippocampal symmetry/asymmetry. In this part feature selection is done according to statistical feature selection test that describe in Feature Selection part.

3.8 Classification

Support vector machine (SVM) is a supervised learning models used for classification and regression analysis with works very well on similar studies [27,28,29]. Linear SVMs search for the optimal hyperplane that separate the dataset to groups, i.e. the hyperplane that makes the maximal margin between groups. For more information about SVM classifiers you can see [26]. We used SVM classifier to classify each test image to normal or patient categories using the selected features (Fig.7). We used our test dataset to evaluate the performance of our classification algorithm.

3.9 Evaluation metrics

To evaluate our detection algorithm performance we calculated specificity, sensitivity and accuracy metrics (equations 19 to 21) for the classifier results. These metrics have been largely used in medical image analysis [25,26].

$$Accuracy = \frac{TP + TN}{TP + FN + TN + FP} \times 100 \quad (19)$$

$$Sensitivity = \frac{TP}{TP + FN} \times 100 \quad (20)$$

$$Specificity = \frac{TN}{FP + TN} \times 100 \quad (21)$$

TP , TN , FP and FN are, respectively, true positive, true negative, false positive and false negative.

3.10 Experimental results

We run our algorithm on 25 segmentation labels of hippocampus on T1-weighted MRI. We divided our image dataset to two subsets; training and test. Training images (12 images, 2 normal and 10 epileptic) were used for feature selection. Test image set consisted of 13 images; 3 normal and 10 epileptic images. All the implementations of this work were implemented in MATLAB platform and run on a Mac operating system.

3.10.1 Features selection

Feature selection consists of two parts. First, feature extraction based on spherical harmonics coefficients. Second, feature extraction based on shape-based features. In each part statistical t-test is used for feature selection. In both parts, the most significant features (associated with p-value < 0.05) is selected. Then combination two selected features create feature vector.

3.10.2 Classification

Leaveoneout cross validation methodology has been applied to divide the test image set to one test image and 12 training for SVM classifier. Having the 18 selected features used in our SVM classifier, the specificity, sensitivity, and accuracy of our detection algorithm were 84%, 100% and 80%, respectively.

3.10.3 Conclusion and future work

Our preparatory results show that combination SPHARM coefficients and shape-based features could be helpful to describe the hippocampus shape deformation and could be used in diagnosis of the temporal lobe epilepsy disease in MRI. Since the dataset we used in our study is formed based on some part of the dataset used in [10,11], not the whole, it is challenging to reach a fair comparison between

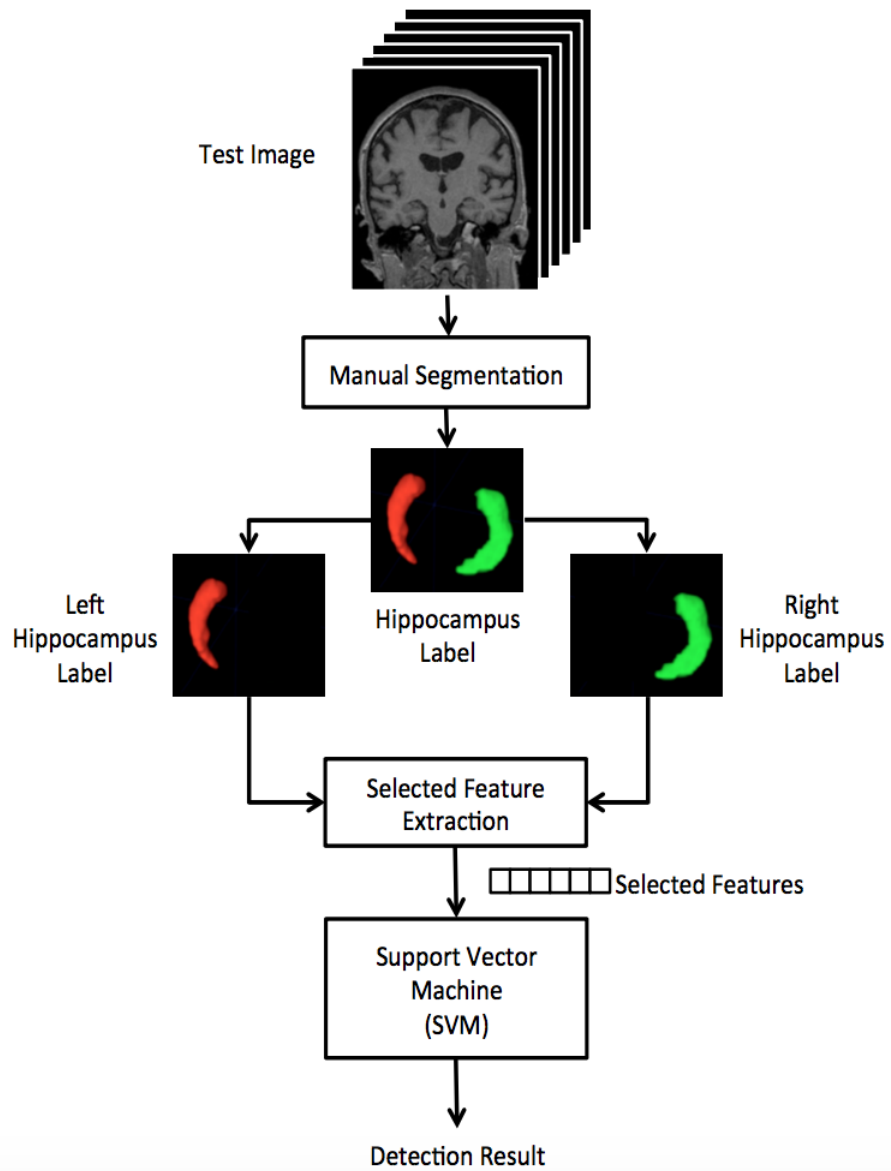


Fig. 7 Classification block diagram

presented results and ours. As an advantage, the complexity of our algorithm is less than the other presented algorithms. In contrast to other work, our method detects the asymmetry in hippocampus structure shape for diagnosis of epilepsy and the preliminary results showed that hippocampal asymmetry detection could be useful for diagnosis of the brain abnormalities such as temporal lobe epilepsy. However, small size of the dataset is a limitation in our work. As future work we are going to increase the number of images in the training and test dataset. We will also compare the results to other reported results in the literature using appropriate statistical tests to examine the significance of the results. We would like to improve the results of our work by adding more shape-based features that are able to significantly separate patients from control groups. It could be also considered to use and evaluate this algorithm for detecting other brain abnormalities.

References

1. Csernansky, John G and Joshi, Sarang and Wang, Lei and Haller, John W and Gado, Mokhtar and Miller, J Philip and Grenander, Ulf and Miller, Michael I, Hippocampal morphometry in schizophrenia by high dimensional brain mapping, *Proceedings of the National Academy of Sciences*, 95, 11406–11411 (1998)
2. Oppenheim, Catherine and Dormont, Didier and Biondi, Alessandra and Lehericy, Stéphane and Hasboun, Dominique and Clémenceau, Stéphane and Baulac, Michel and Marsault, Claude, Loss of digitations of the hippocampal head on high-resolution fast spin-echo MR: a sign of mesial temporal sclerosis., *American journal of neuroradiology*, 19, 457–463, (1998)
3. Convit, A and De Leon, MJ and Tarshish, C and De Santi, S and Tsui, W and Rusinek, H and George, A, Specific hippocampal volume reductions in individuals at risk for Alzheimers disease, *Neurobiology of aging*, 18, 131–138, (1997)
4. Dam, Agnete Mouritzen, *Epilepsy and neuron loss in the hippocampus*, *Epilepsia*, 21, 617–629, (1980)
5. Duvernoy, Henri M, *The human hippocampus: functional anatomy, vascularization and serial sections with MRI*, Springer Science & Business Media (2005),
6. Anstey, KJ and Maller, JJ, The role of volumetric MRI in understanding mild cognitive impairment and similar classifications, *Aging & mental health*, 7, 238–250, (2003),
7. Spherical mapping for processing of 3D closed surfaces, Shen, Li and Makedon, Fillia, *Image and vision computing*, 24, 743–761, (2006)
8. Gerig, Guido and Styner, Martin and Shenton, Martha E and Lieberman, Jeffrey A, Shape versus size: Improved understanding of the morphology of brain structures, *Medical Image Computing and Computer-Assisted Intervention–MICCAI 2001*, 24–32, Springer (2001),
9. Csernansky, John G and Joshi, Sarang and Wang, Lei and Haller, John W and Gado, Mokhtar and Miller, J Philip and Grenander, Ulf and Miller, Michael I, Hippocampal morphometry in schizophrenia by high dimensional brain mapping, *Proceedings of the National Academy of Sciences*, 95, 11406–11411, (1998)
10. Kodipaka, Santhosh and Vemuri, Baba C and Rangarajan, Anand and Leonard, Christiana Morison and Schmallfuss, I and Eisenschenk, S, Kernel fisher discriminant for shape-based classification in epilepsy, *Medical Image Analysis*, 11, 79–90, (2007)
11. Esmaeil-Zadeh, Mohammad and Soltanian-Zadeh, Hamid and Jafari-Khouzani, Kourosh, SPHARM-based shape analysis of hippocampus for lateralization in mesial temporal lobe epilepsy, *Electrical Engineering (ICEE)*, 2010 18th Iranian Conference on, 39–44, IEEE (2010),
12. Shishegar, Rosita and Soltanian-Zadeh, Hamid and Moghadasi, Seyed Reza, Hippocampal shape analysis in epilepsy using Laplace-Beltrami spectrum, *Electrical Engineering (ICEE)*, 2011 19th Iranian Conference on, 1–5, IEEE (2011)
13. Vemuri, Baba C and Guo, Yanlin, Snake pedals: compact and versatile geometric models with physics-based control, *Pattern Analysis and Machine Intelligence*, *IEEE Transactions on*, 22, 445–459, (2000),
14. Vemuri, BC and Ye, J and Chen, Y and Leonard, CM, A level-set based approach to image registration, *Mathematical Methods in Biomedical Image Analysis*, 2000. *Proceedings. IEEE Workshop on*, 86–93, IEEE (2000),

15. Gerig, Guido and Styner, Martin and Jones, D and Weinberger, Daniel and Lieberman, Jeffrey, Shape analysis of brain ventricles using spharm, *Mathematical Methods in Biomedical Image Analysis*, 2001. MMBIA 2001. IEEE Workshop on, 171–178, IEEE (2001),
16. Chaudhury, Baishali and Zhou, Mu and Farhidzadeh, Hamidreza and Goldgof, Dmitry B and Hall, Lawrence O and Gatenby, Robert A and Gillies, Robert J and Weinfurter, Robert J and Drukteinis, Jennifer S, Predicting Ki67% expression from DCE-MR images of breast tumors using textural kinetic features in tumor habitats, *SPIE Medical Imaging*, 9785, 97850T–97850T-7, (2016),
17. Farhidzadeh, Hamidreza and Chaudhury, Baishali and Zhou, Mu and Goldgof, Dmitry B and Hall, Lawrence O and Gatenby, Robert A and Gillies, Robert J and Raghavan, Meera, Prediction of treatment outcome in soft tissue sarcoma based on radiologically defined habitats, *SPIE Medical Imaging*, 9414, 94141U–94141U-5, (2015),
18. Lorensen, William E and Cline, Harvey E, Marching cubes: A high resolution 3D surface construction algorithm, *ACM siggraph computer graphics*, 21, 163–169, (1987),
19. Brechbühler, Ch and Gerig, Guido and Kübler, Olaf, Parametrization of closed surfaces for 3-D shape description, *Computer vision and image understanding*, 61, 154–170, (1995),
20. Shen, Li and Makedon, Fillia, Spherical mapping for processing of 3D closed surfaces, *Image and vision computing*, 24, 743–761, (2006),
21. Andersen, Per and Morris, Richard and Amaral, David and Bliss, Tim and O’Keefe, John, *The hippocampus book*, Oxford University Press, USA (2006),
22. Bribiesca, Ernesto, An easy measure of compactness for 2D and 3D shapes, *Pattern Recognition*, 41, 543–554, (2008),
23. Shen, Liang and Rangayyan, Rangaraj M and Desautels, JE Leo, Application of shape analysis to mammographic calcifications, *Medical Imaging, IEEE Transactions on*, 13, 263–274, (1994),
24. Schölkopf, B and Akritas, Michael G and Politis, Dimitris N, *An introduction to support vector machines*, (2003)
25. Zhu, Wen and Zeng, Nancy and Wang, Ning and others, Sensitivity, specificity, accuracy, associated confidence interval and ROC analysis with practical SAS® implementations, *NESUG proceedings: health care and life sciences*, Baltimore, Maryland, 1–9, (2010)
26. Nascimento, Jacinto C and Marques, Jorge S, Adaptive snakes using the EM algorithm, *Image Processing, IEEE Transactions on*, 14, 1678–1686, (2005),
27. Farhidzadeh, Hamidreza and Goldgof, Dmitry B and Hall, Lawrence O and Gatenby, Robert A and Gillies, Robert J and Raghavan, Meera, Texture Feature Analysis to Predict Metastatic and Necrotic Soft Tissue Sarcomas, *Systems, Man, and Cybernetics (SMC)*, 2015 IEEE International Conference on, 2798–2802, IEEE, (2015),
28. Farhidzadeh, Hamidreza and Kim, Joo Y and Scott, Jacob G and Goldgof, Dmitry B and Hall, Lawrence O and Harrison, Louis B, Classification of Progression Free Survival with Nasopharyngeal Carcinoma Tumors, *SPIE Medical Imaging*, 9785, 97851I–97851I-7, (2016),
29. Farhidzadeh, Hamidreza and Zhou, Mu and Goldgof, Dmitry B and Hall, Lawrence O and Raghavan, Meera and Gatenby, Robert A, Prediction of treatment response and metastatic disease in soft tissue sarcoma, *SPIE Medical Imaging*, 9035, 903518–903518-6, (2014),